JPE 16-2-18

http://dx.doi.org/10.6113/JPE.2016.16.2.572
ISSN(Print): 1598-2092 / ISSN(Online): 2093-4718

A DTC Stator Flux Algorithm for the Performance Improvement of Induction Traction Motors

Pham Van-Tien*, Trillion Q. Zheng†, Zhong-ping Yang*, Fei Lin*, and Viet-dung Do**

*,†School of Electrical Engineering, Beijing Jiaotong University, Beijing, China
**Department of Mechanical Engineering, University of Transport and Communications, Hanoi, Viet Nam

Abstract

In view of the speed control characteristics of induction traction motors and the problems of direct torque control (DTC) algorithms in current applications, this paper presents a DTC algorithm characterized by a symmetrical polygon flux control and a closed loop power control in the constant-torque base speed region and constant-power field-weakening region of induction traction motors. This algorithm only needs to add a stator flux control algorithm to the traditional DTC structures. This has the benefit of simplicity, while maintaining the features of traditional algorithms such as a rapid dynamic response, uncomplicated control circuit, reduced dependence on motor parameters, etc. In addition, it obtains a smoother flux trajectory that is conducive to improvement of the harmonic elimination capability, the switching frequency utilization as well as the torque and power performance in the field-weakening region. The effectiveness and feasibility of this DTC algorithm are demonstrated by both theoretical analysis and experimental results.

Key words: AC motor drives, Direct torque control, Induction rotating machines, Torque control, Traction motor drives

I. INTRODUCTION

Traditional DTC algorithms have weaknesses such as a large torque ripple, inconstant switching frequency, etc. One comparatively effective solution is the use of the Direct Torque Control Space Vector Modulation (DTC-SVM) algorithm. Recent years have seen a continued importance attached to the DTC-SVM algorithm among the improved traditional DTC algorithms [2]-[8]. However, this kind of improved algorithm weakens the simplicity of the traditional DTC structures and in the case of a high power in the mid-high speed ranges and a low switching frequency, the traditional DTC algorithms generally perform better [9], [10].

For alternating current (AC) drive systems using the traditional DTC technologies, the switching frequency of the inverter is closely related to the band of the flux hysteresis controller, the torque hysteresis controller and the motor speed [11]-[13], where the switching frequency is proportional to the motor speed. In other words, the faster the motor speed is, the higher the switching frequency becomes, and it is inversely proportionally to the band of the flux hysteresis controller and the torque hysteresis controller. Furthermore, the stator current harmonic content is proportional to the band of the flux hysteresis controller and the torque hysteresis controller [11], [13]. Different bands of the flux hysteresis controller lead to different flux trajectories [11]. Due to the limitations of the low switching frequency of large-power traction converters [14]-[17], different flux trajectory control modes are used in different speed ranges when DTC algorithms are used for induction traction motors [9].

Since the DTC theory was put forward, four traditional DTC algorithms based on shape of the flux trajectory have been presented, namely, the circular flux trajectory [18], the thirty-corner flux trajectory [19], the eighteen-corner flux trajectory [20] and the hexagonal flux trajectory [21]. The first and the fourth were presented in the 1980s by Japanese Professor I. Takahashi and German Professor M. Dependbrock respectively. The former was mainly applied in small and medium power applications, while the latter was mostly utilized in large-power speed control systems. The second and the third were algorithms proposed on the basis of DTC systems with a hexagonal flux trajectory for reducing current

Manuscript received Aug. 27, 2015; accepted Nov. 23, 2015
Recommended for publication by Associate Editor M. Kazmierkowski.
†Corresponding Author: tqzheng@bjtu.edu.cn
Tel: +86 10 5168 8281, Beijing Jiaotong University
*School of Electrical Engineering, Beijing Jiaotong University, China
**Department of Mechanical Engineering, University of Transport and Communications, Viet Nam

harmonic content. There are principally two symmetric polygonal flux trajectory implementation methods now available. One is based on the interval and switching table and the other is based on the flux hysteresis comparator [10], [19]. However, it is comparatively complicated to use the aforementioned methods to realize other symmetric polygonal flux trajectories when the switching frequency allows. Moreover, it is pointed out in reference [11] that it is theoretically feasible to obtain more polygonal flux trajectories by properly regulating the band of a flux hysteresis controller based on the DTC algorithm with a circular flux trajectory. For example, a circular flux trajectory can be gained by setting the tolerance at its minimum value, and a hexagonal flux trajectory can be realized by setting the tolerance at its maximum value. This algorithm aims at making the flux deviation unaffected by multiple voltage vectors. Therefore, it is difficult to obtain hexagonal, eighteen-corner, thirty-corner and other symmetric polygonal flux trajectories by only changing the band of the flux hysteresis controller.

For a motor running at its base speed, the traditional systems have to use a field-weakening control mode to increase the motor speed. Based on the traditional DTC, reference [22] explained using torque error to regulate a given flux value. However, it is not verified by the square wave modulation algorithm. In reference [23], an over−modulation strategy is put forward based on traditional flux regulation methods for the purpose of expanding the constant torque region and improving the steady-state torque performance. However, the dynamic process neglects torque control and synchronous pulse−width modulation (PWM) modulation is used rather than square wave modulation returns in the steady state. Therefore, it is inappropriate to use these methods in a traction converter that aims at obtaining a constant power in the field-weakening range with square wave modulation.

In view of the above problems, a simple and effective DTC algorithm for induction traction motors is presented for the purposes of smoothening the flux trajectory, fully utilizing the switching frequency and improving the harmonic elimination when the switching frequency allows. This algorithm comprehensively takes into consideration and effectively improves the shortcomings of the above mentioned traditional DTC algorithms. It also extends the stator flux trajectory in the whole-speed range of the existing DTC for induction traction motors to the shape of: circle → symmetric polygon… → symmetric polygon → hexagon. The second section of this paper introduces the basic principles of two typical DTC algorithms, namely the circular flux trajectory and the hexagonal flux trajectory. Then it analyzes and discusses the design and implementation method of the symmetrical polygonal flux trajectory. In the third section, constant-power square wave modulation control algorithm in the field-weakening region is presented and experiment results of the control algorithm are provided in the fourth section. The last section is the conclusion.

II. DTC ALGORITHM WITH THE SYMMETRICAL POLYGONAL FLUX TRAJECTORY

A. Basic DTC Principle

According to the mathematical model of an induction motor, in a static stator coordinate system, the space vector equation of the stator trajectory and electromagnetic torque can be expressed as:

$$\boldsymbol{V}_s = R_s i_s + \frac{d\boldsymbol{\Psi}_s}{dt} \tag{1}$$

$$T_e = \frac{1.5 p_n}{L_\sigma} |\boldsymbol{\Psi}_s \| \boldsymbol{\Psi}_r| \sin\varphi \tag{2}$$

where $\boldsymbol{V}_s$ is the stator voltage space vector, i_s is the stator current space vector, $\boldsymbol{\Psi}_s$ and $\boldsymbol{\Psi}_r$ are the space vectors of the stator flux and the rotor flux, R_s is the stator resistance, L_σ is the sum of the rotor leakage inductance and the stator leakage inductance, p_n is the number of pole pairs, T_e is the electromagnetic torque, and φ is the angle between the stator flux and the rotor flux, namely, the flux angle.

Equation (1) indicates that if the voltage drop $R_s i_s$ of the stator resistance is neglected, the vector $\boldsymbol{\Psi}_s$ of the stator flux will move in the direction of the input voltage space vector at a speed that is proportional to the input voltage value (namely, the voltage acting time), when the input voltage is a non-zero vector. The flux variation is $|\Delta\boldsymbol{\Psi}_s|=\boldsymbol{V}_s\Delta t$. It can be seen in Equation (2) that the rotor flux can be rated as unchanged in the short process. As a result, if the amplitude of the stator flux remains constant, the voltage vector $\boldsymbol{V}_s$ can be used to control the stator flux speed. Then the torque can be quickly controlled by changing the flux angle. Based on the above, references [18, 21] presents the DTC algorithm.

Fig. 1 is a basic control block diagram of the traditional DTC algorithm with circular flux trajectory (Swiching Table Based DTC, ST-DTC) [24], and Fig. 2 shows the distribution of the circular flux trajectory and voltage vector on the static stator coordinate system. This control algorithm uses the checking voltage vector table method to simultaneously control the stator flux and the motor torque, as shown in Table I. θ(i) (i=1 ~ 6) is the flux sector, and C_T and C_Ψ represent the output signals of the torque hysteresis controller and the flux hysteresis controller, respectively (1 indicates increasing the regulating variable, while 0 indicates decreasing the regulating variable). In the DTC algorithm [18] first proposed by Takahashi and Noguchi, two voltage vectors (the reverse voltage vector and the zero voltage vector) are utilized to reduce torque. The inverter requires a low switching frequency, and the inverse voltage vector makes the torque decrease quickly in the medium and high motor speed ranges, which results in a larger torque ripple. Therefore, only the zero voltage vector is used to reduce torque in this paper.

Fig. 3 is a basic control block diagram of a DTC algorithm

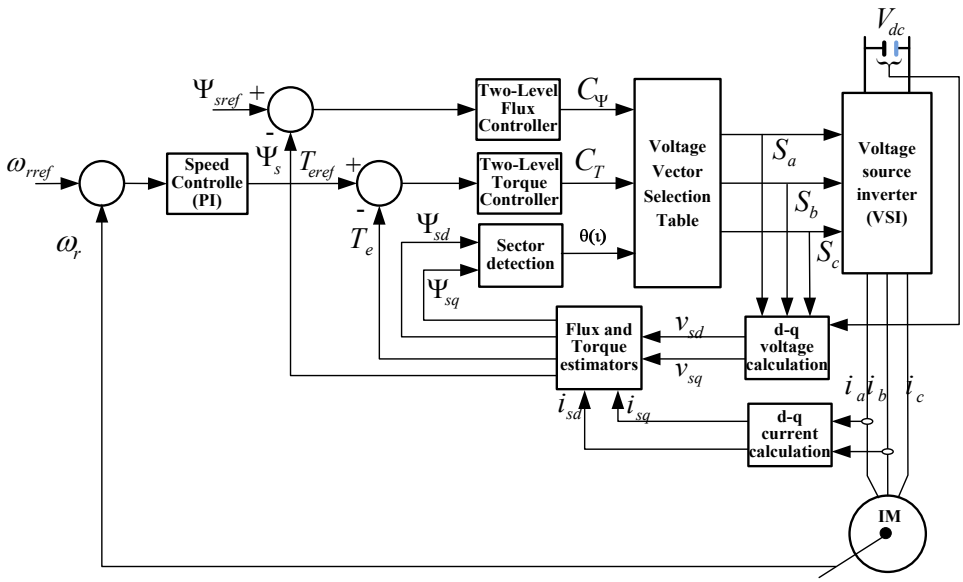

Fig. 1. Block diagram of ST-DTC.

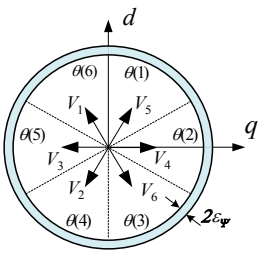

Fig. 2. Circular stator-flux trajectory and space voltage vector.

TABLE I
VOLTAGE VECTOR SELECTION TABLE IN THE CASE OF CLOCKWISE ROTATION

C_T	C_Ψ	θ(1)	θ(2)	θ(3)	θ(4)	θ(5)	θ(6)
1	1	V_4 (100)	V_6 (110)	V_2 (010)	V_3 (011)	V_1 (001)	V_5 (101)
	0	V_6 (110)	V_2 (010)	V_3 (011)	V_1 (001)	V_5 (101)	V_4 (100)
0	1	V_0 (000)	V_7 (111)	V_0 (000)	V_7 (111)	V_0 (000)	V_7 (111)
	0	V_7 (111)	V_0 (000)	V_7 (111)	V_0 (000)	V_7 (111)	V_0 (000)

with the hexagonal flux trajectory (Direct Self Control, DSC) [21], [24]). A stator flux hysteresis controller is used to control 6 non-zero voltage vectors to control the stator flux and make it a hexagon. A torque hysteresis controller is adopted to control the two zero vectors and 6 non-zero voltage vectors of the flux loop, where the former acts to reduce torque while the latter acts to increase torque. Fig. 4 shows the distribution of the hexagonal stator flux and the voltage vector on the static stator coordinate system.

B. Design and Implementation Method of the Symmetric Polygonal Flux Trajectory

Induction traction motors using DTC algorithms must utilize different flux trajectory control modes in the whole-speed range. In order to enhance the switching frequency utilization rate and to improve the sine degree of the stator current, references [10], [19] extend the stator flux trajectory of the existing induction traction motor DTC to the shape of: circle → thirty-corner → eighteen-corner → hexagon in the whole-speed range. However, it is comparatively complicated to achieve more symmetric polygonal flux trajectories to further reduce stator current harmonics, if the switching frequency allows.

The results in reference [11] show that, based on the ST-DTC algorithm, it is theoretically feasible to obtain multiple polygonal flux trajectories such as the hexagon, eighteen-corner, thirty-corner and so on by properly regulating the band of the flux hysteresis controller. However, this kind of trajectory is only approximate since there is an additional side between the two adjacent sectors [11], [13]. Therefore, it shows worse symmetry when compared with the corresponding symmetrical polygonal flux trajectories and requires a greater inverter switching frequency and more switching cycles during implementation [13].

For induction motors, the stator current consists of two components, namely, the active power that generates torque and the excitation of the magnetic field, where the current component that generates torque is determined by the load and the current component that generates excitation is determined by the stator flux trajectory. Thus, the flux trajectory can be designed in terms of the excitation current component performance indicator. In the traditional circular flux trajectory control mode, the flux control focuses on making the flux amplitude fluctuate within the deviation range and on making

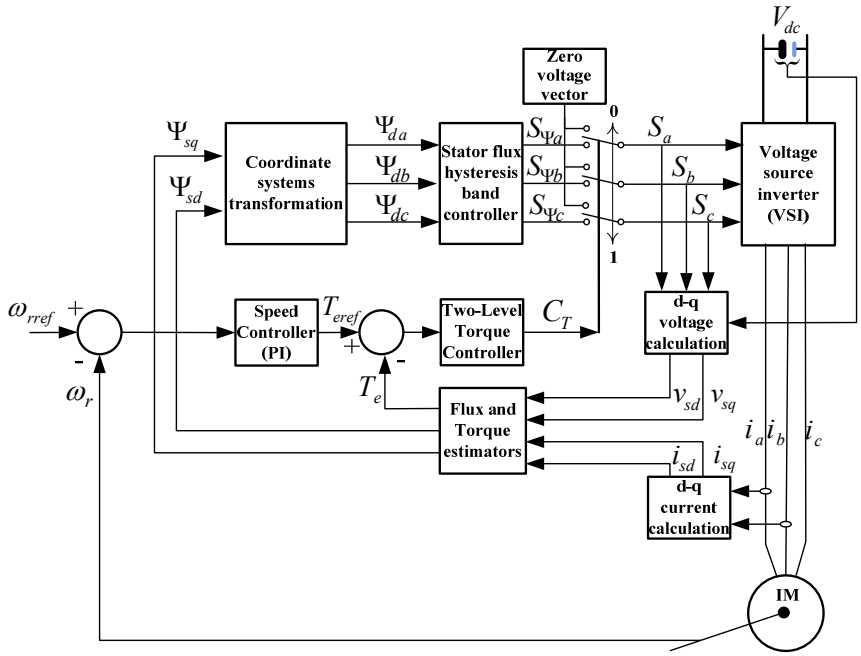

Fig. 3. Block diagram of DSC.

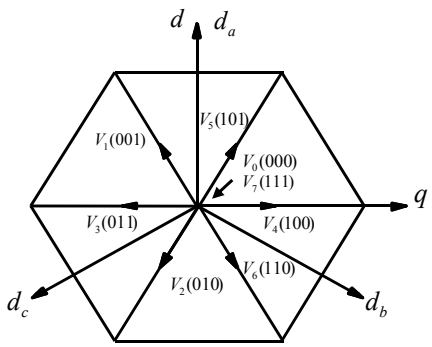

Fig. 4. Hexagonal stator-flux trajectory and space voltage vector.

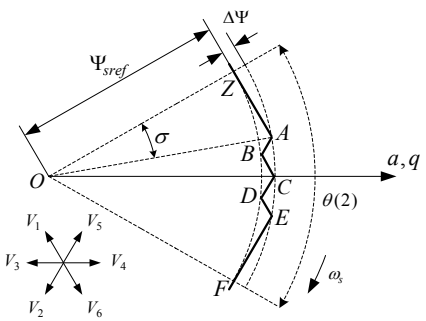

Fig. 5. The second sector of proposed thirty-corner stator-flux trajectory.

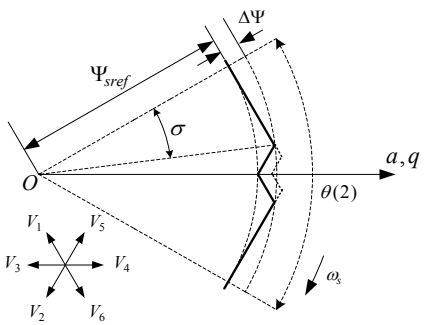

Fig. 6. The second sector of proposed eighteen-corner stator-flux trajectory.

the positive and negative flux deviation values equal, which explains why the excitation current component is characterized by smooth changes. To solve the above problems, the following symmetrical polygon flux trajectory is designed and implemented based on the flux control idea of the ST-DTC algorithm.

Fig. 5 shows the design of a symmetrical polygonal flux trajectory with the second sector of the proposed thirty-corner flux trajectory as an example. In Fig. 5, points Z, B, D and F are on the same circle, while points A, C and E are on another circle. Thus, the flux trajectory has a constant deviation. The smaller $\Delta\Psi$ is, the smaller σ becomes, the larger the number of sides of the symmetrical polygon flux polygon trajectory and the closer the trajectory becomes to a circle. The characteristic of this flux trajectory design method is that only one non-zero voltage vector between two adjacent sectors is selected. That is why there is no additional side. The bigger $\Delta\Psi$ is, the bigger σ becomes, and the smaller the number of sides of the flux trajectory. Then comes the eighteen-corner flux trajectory. The implementation of the trajectory corresponding to the second sector of the eighteen-corner flux trajectory is shown in Fig. 6.

When $\Delta\Psi$ is at its maximum and $\sigma=\pi/6$, a hexagonal flux trajectory is obtained. It can be seen in Fig. 6 that there are a lot of other eighteen-corner flux trajectories that can be selected

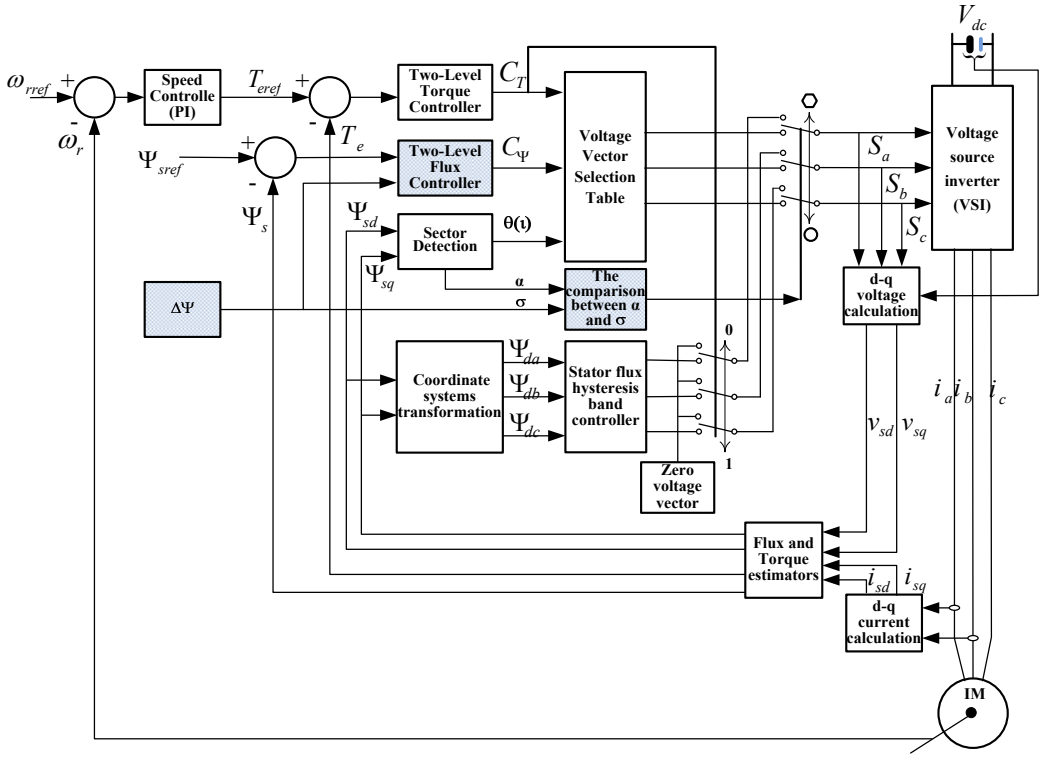

Fig. 7. Structure of the proposed DTC with the symmetrical polygonal stator-flux trajectory

between the eighteen-corner flux trajectory and the hexagonal flux trajectory. In addition, when switching trajectories are required, the two can be switched directly instead of gradually reducing σ (the dashed line segment in Fig. 6). In fact, this method makes the current waveform worse and the switching frequency shows no advantages since the number of voltage vectors to be switched remains unchanged [13].

In Fig. 5, the middle trajectory (ABCDE segment in Fig. 5) in the sector is achieved by alternatively switching $\boldsymbol{V}_2$ and $\boldsymbol{V}_6$, and the flux deviation in this area is fixed. The other two flux trajectories (ZA and EF segments in Fig. 5) in the sector are realized by $\boldsymbol{V}_2$ and $\boldsymbol{V}_6$, respectively. When the shape of the flux trajectory is determined, $\Delta\Psi$ and σ are also determined. It can be determined from the control algorithm of the traditional circular and hexagonal flux trajectories in the previous section that design of the flux trajectory can be obtained by combining the two flux trajectory control methods. This means that the middle ABCDE segment trajectory can be implemented by using the ST-DTC algorithm when the band of the flux hysteresis controller is set as [$-\Delta\Psi$, 0] and the other two ZA and EF trajectories can be implemented with the DSC algorithm. This approach is simple and it is easy to realize multiple polygonal flux trajectories.

Based on the above analysis, compared with the design method of the traditional circular flux trajectory, the design method of this flux trajectory maintains the feature of keeping the flux trajectory deviation unchanged and solves the problems in the existing references. As a result, it is more suitable for systems using multi-flux trajectory control mode.

Fig. 7 shows the structure of the proposed DTC with the symmetrical polygonal flux trajectory. It is obtained by adding a simple stator flux control algorithm to the combination of Fig. 1 and Fig. 3. The "$\Delta\Psi$" module determines the number of sides of the flux trajectory. $\Delta\Psi$ is used to calculate σ. Then the value of σ is compared with α of the stator flux in each sector to determine the switching time between the circular flux trajectory and the hexagonal flux trajectory.

III. Constant Power Closed-Loop Control Algorithm in the Field-Weakening Region

With an increase of the motor speed, the stator voltage also increases. In addition, when the motor reaches its base speed, the direct current (DC) voltage is fully used. For traditional systems to further increase the motor speed, the field-weakening control must be conducted. It is a particular issue to use the field-weakening control mode in motors with a speed higher than the base speed in large-power applications such as traction drive systems. After entering the field-weakening region, in order to maximally increase the utilization of the DC bus voltage, a traction inverter usually conducts square wave modulation on the condition of a constant power. Since it is impossible to control torque by changing the output voltage vector in the situation of square wave modulation, the torque control depends on the control of

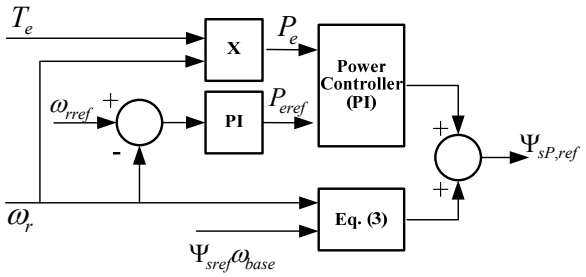

Fig. 8. Reference of stator flux controller in weakening region module.

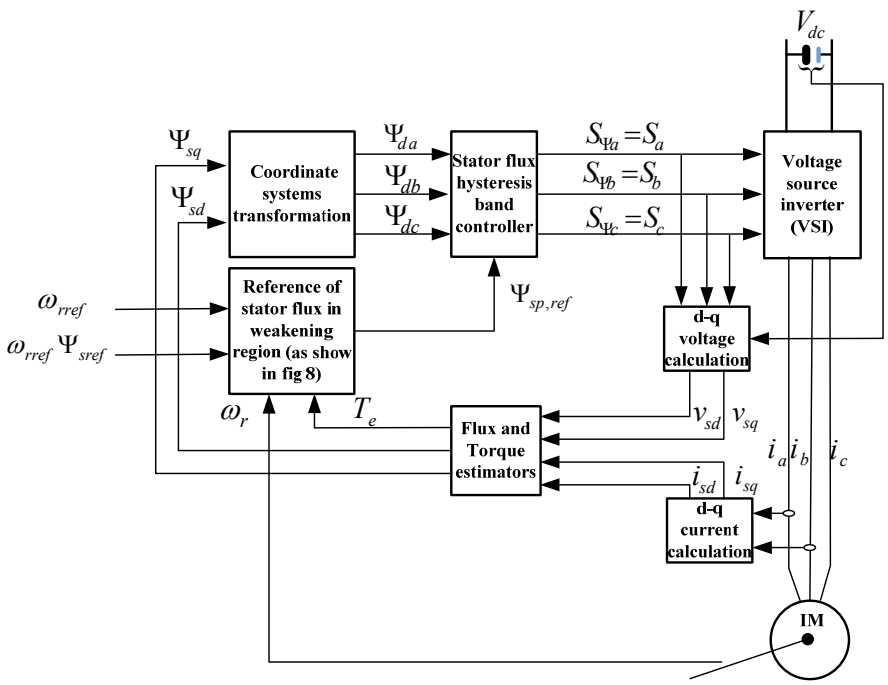

Fig. 9. Structure of the DTC in weakening region.

the flux trajectory and the control performance rests with the performance of the flux regulator. Therefore, operation in the field-weakening region is quite different from that in the constant flux region. First, it is constant power regulation rather than constant torque regulation that is operating in the field-weakening region. Second, full voltage works in the field-weakening region, leaving no time for the zero voltage vector, while the non-zero voltage vector is working in the entire sector. This brings two characteristics of the field-weakening region: 1) an increase of speed, namely, an increase of the stator frequency. The accelerating rotation of the stator flux space vector relies on the decreasing given flux value, namely, the steady-state field weakening; 2) the regulation of torque depends on the dynamic regulation on a given value of the hexagonal flux instead of on limiting the torque to within the tolerance by the alternating operating voltage vector and the zero voltage vector or the reverse operating voltage vector.

Fig. 8 shows the given flux regulation module in the field-weakening region. The given torque value from the PI regulation of the speed controller works as a given value for the power in the field-weakening region. As a result, the power in this region is controlled with the power controller. The actual value P_e is obtained through a calculation of the torque T_e of the motor module and the speed ω_r of the detection. The PI regulation of the power controller is obtained by comparing the given power value with the actual power value, and output of the power controller is the dynamic component Ψ_{sT} of the given flux value. As a result, the torque is controlled in the field-weakening region. The steady-state component $\Psi_{s\omega}$ of the given stator flux value meets the requirements of motor speed in the field-weakening region and can be obtained via equation (3) with the traditional field-weakening method.

$$\Psi_{s\omega}=\frac{\Psi_{sref}\omega_{base}}{\omega_r} \tag{3}$$

In this equation, Ψ_{sref} is the reference value (Wb) of the stator flux in the contast torque region, ω_{base} is the motor speed (rad/s) when the system enters the constant power region and ω_r is the motor speed (rad/s).

Fig. 9 is a principle block diagram of the DTC in the

TABLE II
EXPERIMENT PARAMETERS

Direct current V_{dc}	300 (V)
Reference stator flux Ψ_{sref}	1 (Wb)
Reference torque T_{eref}	10 (Nm)
DSP sampling time Ts	50 (μs)

field-weakening region. In the field-weakening region, the stator flux rotates according to the hexagonal trajectory with the full voltage operating, and the torque control relies on the dynamic regulation of the given hexagonal flux value. Therefore, this block diagram does not show contents such as the control stator flux of the circular trajectory in the base speed range or the selection of the torque hysteresis controller and the zero voltage vector, etc. However, it shows that the given flux control module is added to control the band of the stator hysteresis controller in the DSC algorithm, and that the output signal of the stator hysteresis controller directly forms the inverter switching signal to control the motor speed. In addition, the torque and the power meet the requirements.

IV. EXPERIMENTAL RESULTS

Small power induction motors are used to verify the principle in this paper. The motor parameters include: the stator resistance R_s=1.517 (Ω), the rotor resistance R_r=1.483 (Ω), the stator leakage inductance L_{ls}=2 (mH), the rotor leakage inductance L_{lr}=2 (mH), the mutual inductance L_m=172 (mH), the number of pole pairs n_p=2, and the rotational inertia j=0.83 (kg.m^2). Table II shows the experiment parameters from which the motor's base speed range (0 ~ 200 rad/s) can be calculated.

In order to verify the control algorithm of the improved flux trajectory design, experiments on two control algorithms are conducted by changing the band of the flux hysteresis controller under the same experimental conditions. For ease of comparison and distinction, the two algorithms are expressed as followings:

1) DTC1: the traditional DTC algorithm with the circular flux trajectory.

2) DTC2: the DTC algorithm with the symmetrical flux trajectory proposed in this paper.

Based on the above, the effectiveness of the constant-power closed-loop control in the field-weakening region is verified. Experiments are conducted on the two control algorithm with motor speeds from 0 to 500 rad/s. The reference algorithms are listed below:

1) DTC3: the multi-flux trajectory control mode and the traditional field-weakening control algorithm of the open loop power [23].

2) DTC4: the multi-flux trajectory control mode and the traditional field-weakening control algorithm of the closed-loop power proposed in this paper.

The multi-flux trajectory control mode is used in the base speed range. It is designed to achieve the flux trajectory shapes: sixty-six-corner → fifty-four-corner → forty-two-corner → thirty-corner → eighteen-corner → hexagon.

Fig. 10 shows experimental results of the stator-flux trajectories of DTC1 and DTC2 with different bands of the flux hysteresis controller. It can be seen from Fig. 10 that the smaller the flux band is set, the larger the number of sides of the flux trajectories, and the closer the shape is to a circle. Further, Table III shows that the harmonic elimination capability is improved. However, the switching frequency becomes higher at the same time [11]-[13].

It can be seen from Fig. 10(a) that an additional side (indicated as a circle in the Figure) appears in the experimental result of the DTC1 algorithm, which is located between any two adjacent sectors in the flux trajectory, which is correspondingly obtained from each flux band. Apparently, this method of changing the band of the flux hysteresis controller can only realize approximate flux trajectories of one sort such as the sixty-six-corner, fifty-four-corner, forty-two-corner, thirty-corner, eighteen-corner, hexagon and the like. However, they have poor symmetry. Moreover, it can be calculated that when the flux trajectory deviation gradually changes from small to large, the average flux switching frequency is correspondingly $13f_e$, $11f_e$, $9f_e$, $7f_e$, $5f_e$ and $3f_e$, where f_e is the stator flux frequency [13]. Meanwhile, using the DTC2 algorithm with the same setting of the flux deviation, symmetrical polygonal flux trajectories such as the sixty-six-corner, fifty-four-corner, forty-two-corner, thirty-corner, eighteen-corner, hexagon and so on are obtained, as shown in Fig. 10(b). The symmetry of the stator flux trajectory in DTC2 is better than that in DTC1. Thus, from Table III, it can be seen that DTC2 is better for suppressing current harmonics when compared with DTC1. When the flux trajectory deviation gradually changes from small to large, the average flux switching frequency is correspondingly $12f_e$, $10f_e$, $8f_e$, $6f_e$, $4f_e$ and $2f_e$, which reduces the requirement of the DTC1 algorithm in terms of the flux switching frequency, improves the switching frequency utilization and is of great significance to motor traction with limited switching frequency resources.

Fig. 11(a) and Fig. 11(b) show experimental results of the flux trajectories of DTC3 and DTC4, respectively. They show that the stator flux motions in a trajectory of multiple shapes in the constant-torque base speed region and it moves in a trajectory where the hexagon shape and the amplitude gradually reduce with an increase of speed in the field-weakening region.

The motor power, motor torque, motor speed, stator phase current and phase voltage of DTC3 and DTC4 are separately shown in Fig. 12(a) and Fig. 12(b). The Fig. 12 indicates that in the field-weakening square wave modulation region, the DTC3 algorithm can meet the requirement of motor speed, since it only regulates the motor speed. However, it cannot

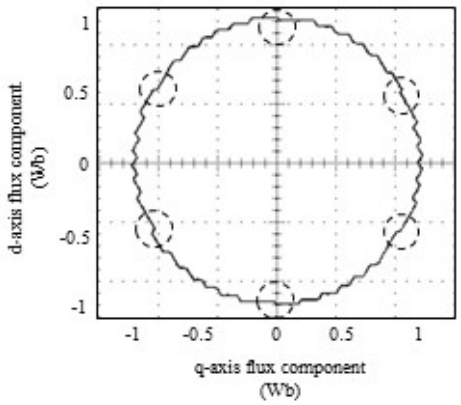

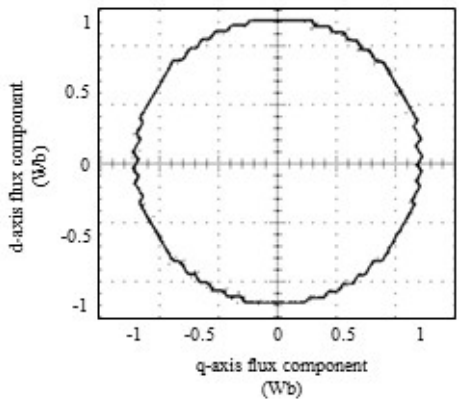

ΔΨ=0.028

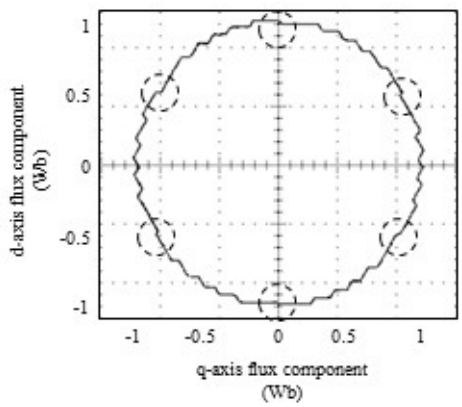

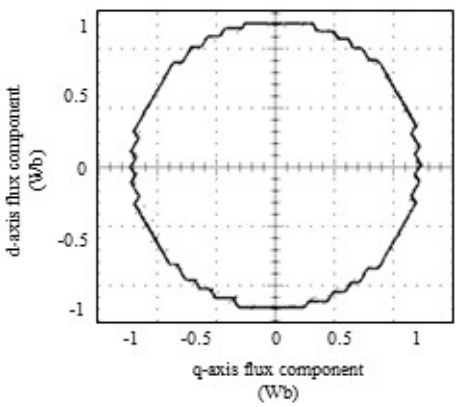

ΔΨ=0.033

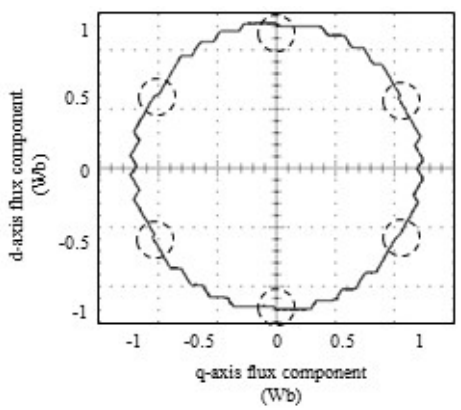

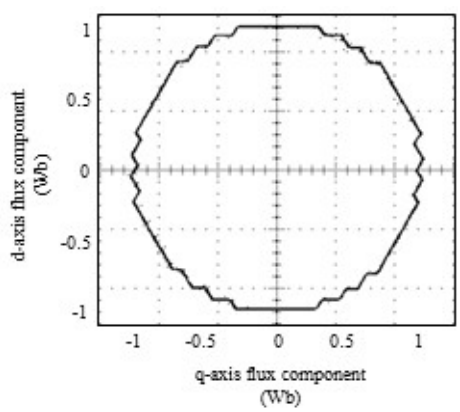

ΔΨ=0.042

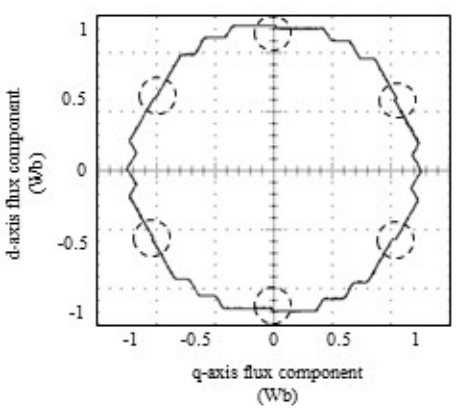

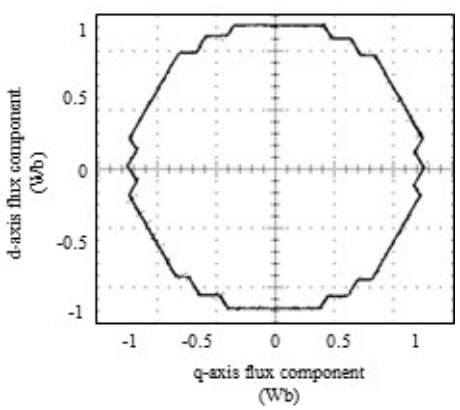

ΔΨ=0.056

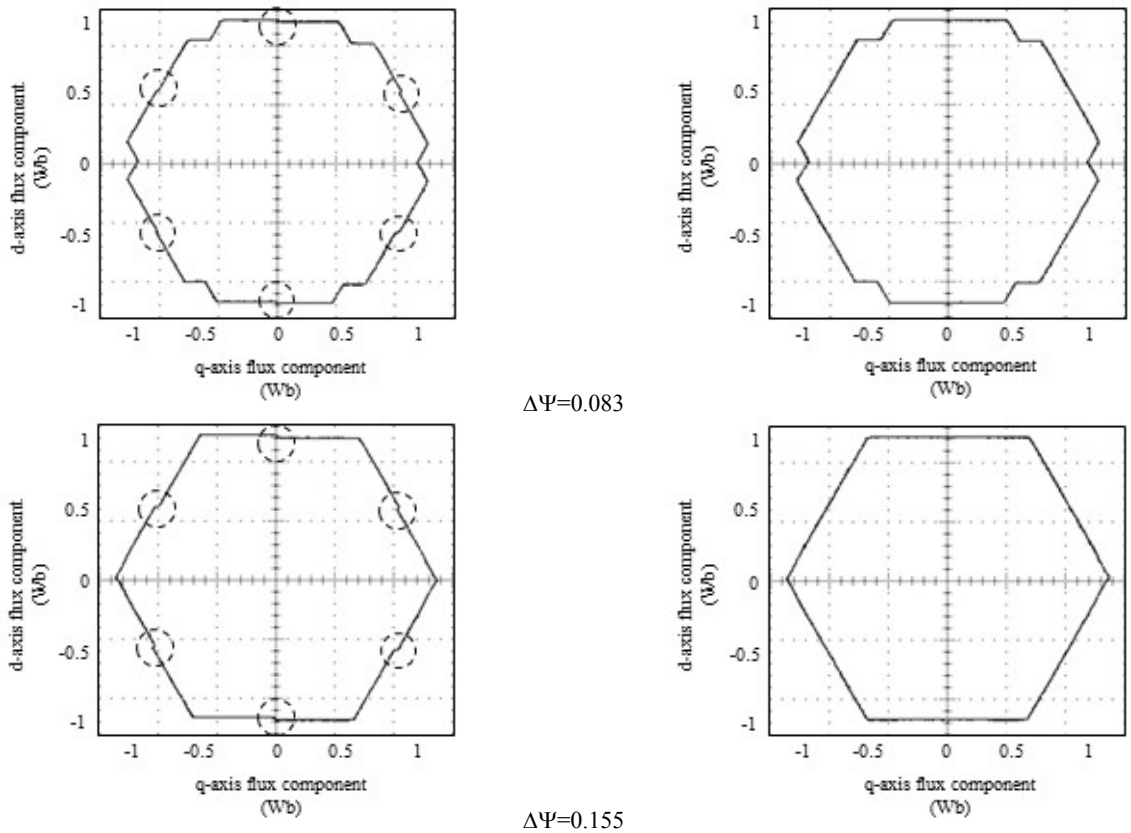

(a): DTC1. (b): DTC2.

Fig. 10. Experimental results of stator-flux locus with different flux hysteresis band magnitude with DTC1 and DTC2.

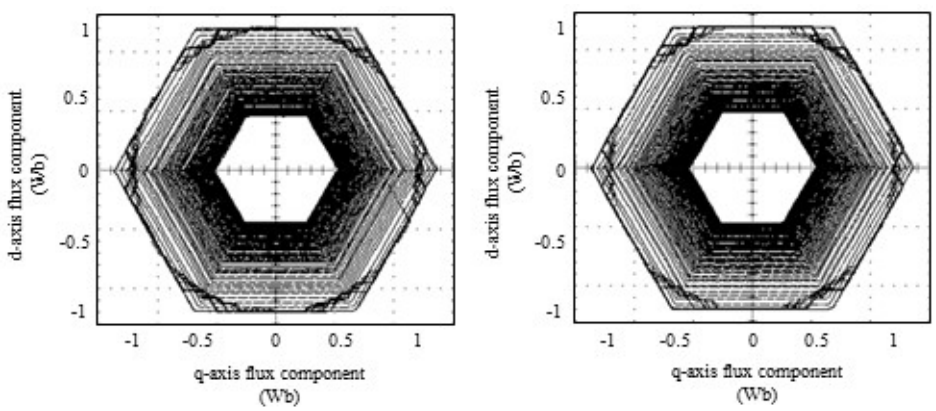

(a) DTC3. (b) DTC4.

Fig. 11. Experimental results of stator-flux locus with DTC3 and DTC4.

TABLE III

TOTAL HARMONIC DISTORTION FACTOR OF MOTOR CURRENT WHEN USE DTC1 AND DTC2 WITH THE MOTOR SPEED OF 160 RAD/S

The control algorithm	Bands of flux hysteresis controller: ΔΨ					
	0.155	0.083	0.056	0.042	0.033	0.028
	THD (Total harmonic distortion factor) (%)					
DTC1	6.494	3.710	2.587	2.053	1.634	1.432
DTC2	6.450	3.676	2.574	1.978	1.606	1.415

guarantee a constant motor power, and the motor power, motor torque and stator phase current have a poor smoothness. When approaching its given speed, the motor enters a steady state, but in a comparatively slow way, which costs about 3.6 s. The DTC4 algorithm meets the motor speed requirement by changing the stator flux amplitude. It also controls the motor torque by regulating the stator flux amplitude in the dynamic process and gains a generally constant motor power. In addition, the motor torque and the stator phase current fluctuate in a comparatively uniform way. When approaching its given speed, the motor reaches the steady state faster, costing about 2.65 s. Therefore, the control performance of the DTC4 algorithm with the closed-loop power is superior to

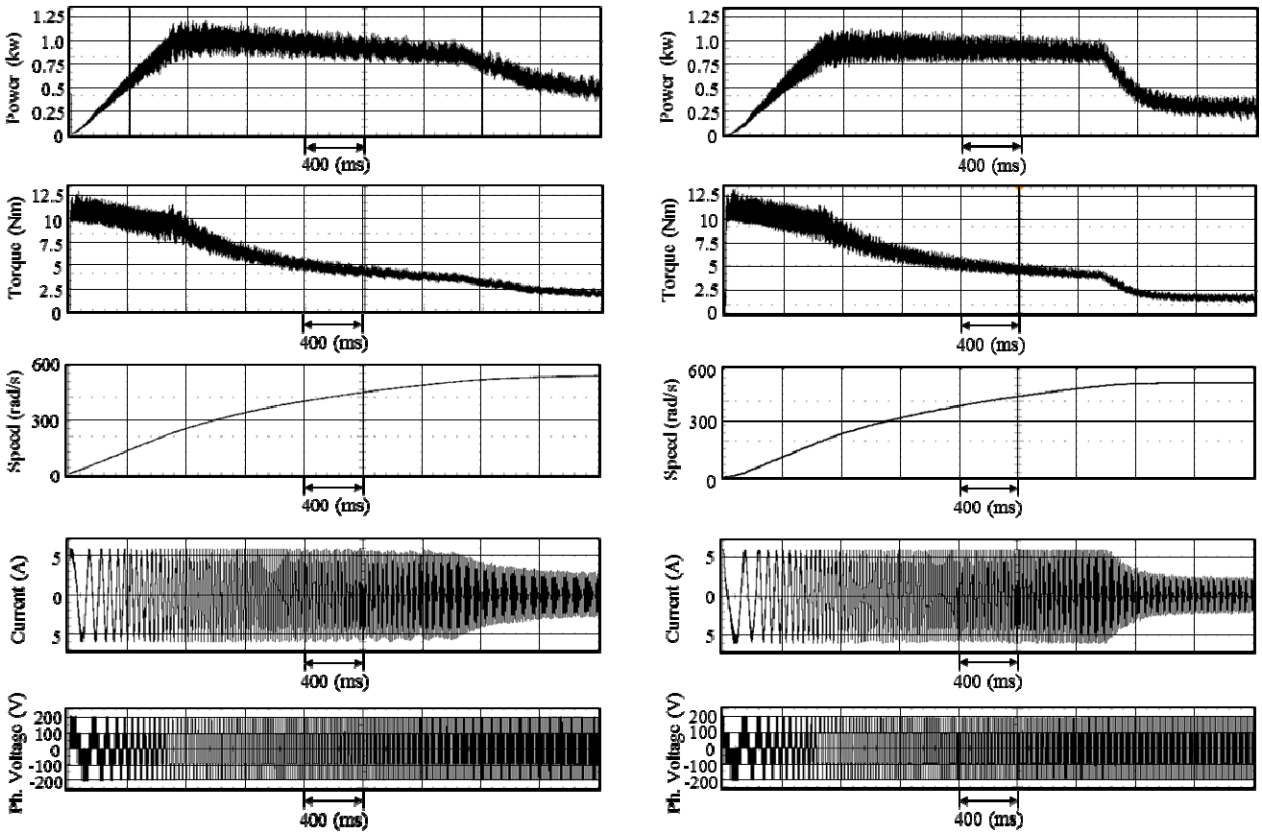

(a) DTC3. (b) DTC4.

Fig. 12. Experimental results of output power, output torque, motor speed, stator phase current, and stator phase voltage with DTC3 and DTC4.

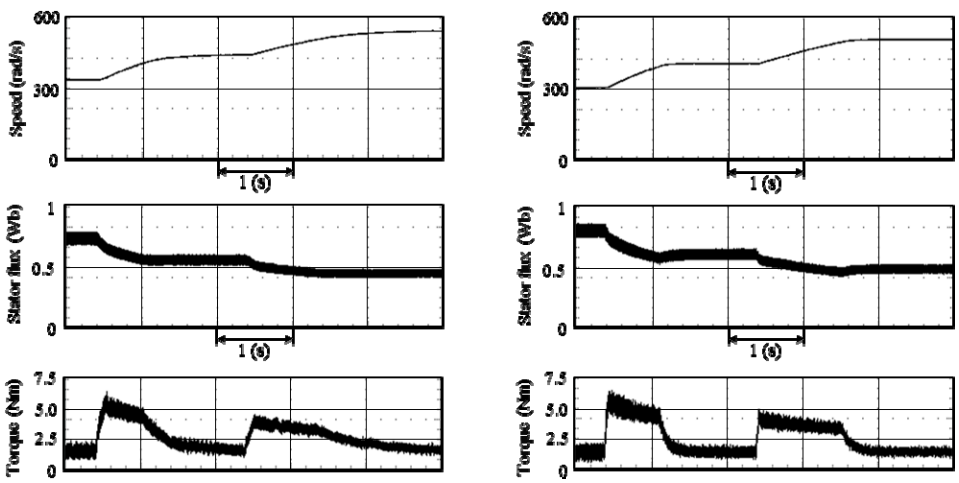

(a) DTC3. (b) DTC4.

Fig 13. Experimental results of motor speed, stator flux, and output torque with DTC3 and DTC4 in field weakening range.

that of the DTC3 algorithm.

In order to compare the dynamic responses of DTC3 and DTC4, Fig .13 shows experimental results when the rotor speed is accelerated from 300 rad/s to 400 rad/s, and then from 400 rad/s to 500 rad/s, continuously. This figure shows that due to the contribution of the dynamic component control of the stator flux, DTC4 can achieve a fast torque response, and reach the steady-state quickly. In DTC3, the accuracy of the speed control is low due to the open-loop controller. Therefore, the actual speed is larger than the speed reference. As a result, the actual amplitude of the stator flux is lower than its reference value. This phenomenon can be observed as shown in Fig. 13(a).

V. CONCLUSION

With induction traction motors as the research object and the traditional DTC technologies as the research methods, a DTC algorithm with an improved flux trajectory and a constant power in the field-weakening region is elaborated on in this paper. This algorithm is characterized by the following:

(1) When compared with traditional DTC algorithms, the proposed symmetrical flux trajectory design method maintains the advantage of keeping the flux trajectory deviation unchanged. It also improves the control effect on the flux trajectory symmetry, reduces the requirement on the flux switching frequency and increases the utilization of the switching frequency. In comparison with the current design methods of the symmetrical polygon flux trajectory, when the switching frequency allows, this method apparently shows increased simplicity and is more suitable for practice design if more symmetrical polygon flux trajectories are to be obtained. When using DTC technology, induction traction motors need to control the flux trajectory in different regions. As a result, a smooth gradual transition from the symmetrical polygonal flux trajectory mode to the hexagonal flux trajectory mode is achievable with an increase of the motor speed. In this paper, the multi-flux trajectory control mode is sixty-six-corner → fifty-four-corner → forty-two-corner → thirty-corner → eighteen-corner → hexagon.

(2) When the traction motor conducts square wave modulation in the field-weakening region, the stator flux can be controlled with the traditional field-weakening control method in combination with the closed-loop power control so as to improve the torque and power performance.

(3) The proposed algorithm possesses the features of the traditional DTC algorithm, such as simplicity of the control structure, insensitivity to motor rotor parameters, etc., because this algorithm only adds a stator flux regulation algorithm to the traditional DTC structure.

Although it is only verified by experiments on small power motors, the algorithm proposed here can be applied to small and medium power industrial systems and large power alternating traction drive systems.

REFERENCES

[1] T. G . Hableter, F. Profumo, M. Pastorelli, and L. M. Tolbert, "Direct torque control of induction machines using space vector modulation," *IEEE Trans. Ind. Appl.*, Vol. 28, No. 5, pp. 1045-1053, Sep./Oct. 1992.

[2] F. M. Borujeni and M. Ardebili, "DTC-SVM control strategy for induction machine based on indirect matrix converter in flywheel energy storage system," in *Proc. PEDSTC*, pp. 352-357, 2015.

[3] M. Dybkowski and K. Szabat, "Direct torque control of induction motor drive system with adaptive sliding-mode neuro-fuzzy compensator," in *Proc. ICIT*, pp. 714-719, 2015.

[4] H. Moghbeli, M. Zarei, and S. S. Mirhoseini, "Transient and steady states analysis of traction motor drive with regenerative braking and using modified direct torque control (SVM-DTC)," in *Pro*. PEDSTC, pp. 615-620, 2015.

[5] D. Stando and M. P. Kazmierkowski, "Novel speed sensorless DTC-SVM scheme for induction motor drives," in *Proc. CPE*, pp. 225-230, 2013.

[6] Y. Wang and Z. Q. Deng, "A position sensorless method for direct torque control with space vector modulation of hybrid excitation flux-switching generator," *IEEE Trans. Energy Convers.*, Vol. 27, No. 4, pp. 912-921, Dec. 2012.

[7] Z. F. Zhang, R. Y. Tang, B. D. Bai, and D. X. Xie, "Novel direct torque control based on space vector modulation with adaptive stator flux observer for induction motors," *IEEE Trans. Magn.*, Vol. 46, No. 8, pp. 3133-3136, Aug. 2010.

[8] K. B. Lee and F. Blaabjerg, "Sensorless DTC-SVM for induction motor driven by a matrix converter using a parameter estimation strategy," *IEEE Trans. Ind. Electron*., Vol. 55, No. 2, pp. 512-521, Feb. 2008.

[9] A. Steimel, "Direct self control and synchronous pulse techniques for high-power traction inverters in comparison," *IEEE Trans. Ind. Electron.*, Vol. 51, No. 4, pp. 810-820, Aug. 2008.

[10] Y. H. Leo, "Research on key problems of direct torque control in electric traction system," D Thesis, Southwest Jiaotong University, China, 2013.

[11] D. Casadei, D. Grandi, G. Serra, and A. Tani, "Effects of flux and torque hysteresis band amplitude in direct torque control of induction machines," in *Proc. IECON*, pp. 299-304, 1994.

[12] M. P. Kazmierkowski and A. B. Kasprowicz, "Improved direct torque and flux vector control of PWM inverter-fed induction motor drives," *IEEE Trans. Ind. Electron.*, Vol. 42, No. 4, pp. 344-349, Aug. 1995.

[13] J. K. Kang and S. K. Sul, "Analysis and prediction of inverter switching frequency in direct torque control of induction machine based on hysteresis bands and machine parameters," *IEEE Trans. Ind. Electron.*, Vol. 48, No. 3, pp. 545-553, Jun. 2001.

[14] W. S. Song, J. P. Ma, L. Zhou, and X. Y. Feng, "Deadbeat predictive power control of single-phase three-level neutral-point-clamped converters using space-vector modulation for electric railway traction," *IEEE Trans. Power Electron.*, Vol. 31, No. 1, pp. 721-732, Jan. 2016.

[15] S. K. Sahoo and T. Bhattacharya, "Rotor flux oriented control of induction motor with synchronized sinusoidal PWM for traction application," *IEEE Trans. Power Electron.*, Vol. 31, No. 6, pp. 4429-4439, Jun. 2016.

[16] L. T. Zhao, L. J. Diao, Z. Zhang, and Z. G. Liu, "Discrete-time current controller for induction motors at low switching frequency," in *Proc. the CSEE*, Vol. 34, No. 21, pp. 3456-3466, Jul. 2014.

[17] M. L. Zhou, X. J. You, and C. C. Wang, "Vector control of driving system of locomotive," *Transactions of China Electrotechnical Society*, Vol. 26, No. 9, pp. 110-115, Sep. 2011.

[18] I. Takahashi and T. Noguchi, "A new quick-response and high efficiency control strategy of an induction motor," *IEEE Trans. Ind. Appl.*, Vol. 22, No. 5, pp. 820-827, Sep./Oct. 1986.

[19] Y. H. Leo, X. Y. Feng, and Z. Wang, "Research on harmonic elimination in low switching frequency based on direct self control," *Transactions of China Electrotechnical Society*, Vol. 27, No. 8, pp. 126-132, Aug. 2012.

[20] A. Steimel, "Further development of direct self control for

application in electric traction," in *Proc*. *ISIE*, pp. 180-185, 1996.
[21] M. Depenbrock, "Direct self control(DSC) of Inverter Fed Induction Machine," *IEEE Trans. Power Electron.*, Vol. 3, No. 4, pp. 420-429, Jul. 1988.
[22] D. Casadei, G. Serra, A. Stefani, A. Tani, and L. Zarri, "DTC drives for wide speed range applications using a robust flux-weakening algorithm," *IEEE Trans. Ind. Electron.*, Vol. 54, No. 5, pp. 2451-2461, Oct. 2007.
[23] A. B. Jidin, N. R. B. N. Idris, A. H. B. M. Yatim, M. E. Elbuluk, and T. Sutikno, "Wide-speed high torque capability utilizing overmodulation strategy in DTC of induction machines with constant switching frequency controller," *IEEE Trans. Power Electron.*, Vol. 27, No. 5, pp. 2566-2575, May 2012.
[24] G. S. Buja and M. P. Kazmierkowski, "Direct torque control of PWM inverter-fed AC motors-a survey," *IEEE Trans. Ind. Electron.*, Vol. 51, No. 4, pp. 744-757, Aug. 2004.

Pham Van-Tien was born in Haiduong, Vietnam, in 1981. He received his B.S. degree in Mechanical Engineering from the University of Transport and Communications, Hanoi, Vietnam, in 2004; and M.S. degree in Electrical Engineering from Southwest Jiaotong University, Chengdu, China, in 2008. He is presently a Ph.D. Research Fellow in the School of Electrical Engineering, Beijing Jiaotong University, Beijing, China. His current research interests include the digital control and modulation methods of DC-AC and AC-DC-AC railway traction drive systems.

Trillion Q. Zheng (M'06-SM'07) was born in Jiangshan, Zhejiang Province, China, in 1964. He received his B.S. degree in Electrical Engineering from Southwest Jiaotong University, Sichuan, China, in 1986; and his M.S. and Ph.D. degrees in Electrical Engineering from Beijing Jiaotong University, Beijing, China, in 1992 and 2002, respectively. He is presently a University Distinguished Professor at Beijing Jiaotong University. He directs the Center for Electric Traction, sponsored by the Ministry of Education, China. His current research interests include the power supplies and AC drives of railway traction systems, high performance and low loss power electronics systems, and power quality corrections. He holds 24 Chinese patents, and has published over 80 journal articles and more than 120 technical papers in conference proceedings. From 2003 to 2011, he served as Dean in the School of Electrical Engineering, Beijing Jiaotong University. He is presently serving as the Deputy Director of the Beijing Society for Power Electronics. He was a laureate of the Zhongda Scholars for Power Electronics and Motor Drives of the Delta Environmental and Educational Foundation and received other provisional and national awards.

Zhong-ping Yang was born in Chongqing, China, in 1971. He received his B.S. degree in Electrical Engineering from the Tokyo University of Mercantile Marine, Tokyo, Japan, in 1997; and his M.S. and Ph.D. degrees in Electrical Engineering from the University of Tokyo, Tokyo, Japan, in 1999 and 2002, respectively. He is presently working as a Professor in the School of Electrical Engineering, Beijing Jiaotong University, Beijing, China. His current research interests include high-speed rail systems, traction and regenerative braking technologies, and wireless power transfer for light rail vehicles.

Fei Lin was born in Shandong Province, China, in 1975. He received his B.S. degree from Xi'an Jiaotong University, Xi'an, China, in 1997; his M.S. degree in Electrical Engineering from Shandong University, Shandong, China, in 2000; and his Ph.D. degree from Tsinghua University, Beijing, China, in 2004. In 2004, he became a Lecturer in School of Electrical Engineering, Beijing Jiaotong University, Beijing, China, where he is presently working as an Associate Professor. He is also a Member of the IEEE. His current research interests include power electronics and motor control.

Viet-dung Do was born in Hanoi, Vietnam. He received his B.S., M.S. and Ph.D. degrees in Mechanical Engineering from the University of Transport and Communications, Hanoi, Vietnam, in 1979, 1998 and 2003, respectively. He is presently working as a Professor in the Department of Mechanical Engineering, University of Transport and Communications. His current research interests include control methods for AC-AC, DC-AC, and AC-DC-AC railway traction drive systems.